

Interactions in dye-microcavity photon condensates and the prospects for their observation

R. A. Nyman*

*Centre for Cold Matter, Blackett Laboratory, Imperial College London,
Prince Consort Road, SW7 2BW, United Kingdom*

M. H. Szymańska

Department of Physics, University of Warwick, Coventry CV4 7AL, United Kingdom

(Dated: Wednesday 15th June, 2022)

Photon do not normally Bose condense as they do not conserve particle number. They are massless and non-interacting. However, by confining them in a cavity and using a dye medium to help them thermalise, a photon Bose-Einstein condensate has recently been created. The next quest is to demonstrate superfluid behaviour, which depends on the strength of dye-mediated photon interactions: currently unknown. We propose an experimental set up to measure the interactions based on detecting the subtle effects in the photoluminescence spectrum of the photon condensate. Considering realistic parameters and experimental resolution we estimate that this method can resolve dimensionless interaction parameters of order 10^{-5} , two orders of magnitude below current estimates. Thus we expect that this technique will lead to accurate measurements of the interactions in photon condensates.

Bose-Einstein condensation is usually thought of as a low-temperature phenomenon. However, Klaers *et al* made the first room-temperature Bose-Einstein condensate (BEC) [1] by confining photons in a cavity filled with fluorescent dye to provide the photons with an effective mass and to allow photon thermalisation at fixed photon number. Under well-chosen experimental conditions[2, 3], the photons come into thermal equilibrium with a dye, and the evidence for the Bose-Einstein condensation transition was strong. Due to the room-temperature operation and relatively simple experimental set up in comparison to other lower temperature condensates this system offers now an ideal playground to study macroscopic quantum systems.

While Bose-Einstein condensation was initially proposed in the context of non-interacting Bose gas, the interactions which make this phase transition experimentally possible lead to a plethora of collective quantum phenomena. For example, bosons with repulsive interactions, such as liquid helium-4 and atomic gases, make superfluids while attractive interactions lead to pairing of fermions and superconductivity, superfluidity of helium-3, and molecular BECs in trapped gases. The interactions in exciton-polariton condensates[4] play a crucial role in the observed excitation spectra[5, 6] and superfluid behaviour such as quantised vortices[7] and persistent currents[8, 9]. A superfluid description of light, setting aside the thermalisation process, was first proposed by R. Chiao[10–12], which follows on from earlier descriptions of inhomogeneous gain media in optical cavities[13–15]. The suggestion was to use dilute vapours of alkali metals as a non-linear medium, together with an optical

resonator to constrain the dispersion relation of the light.

In the context of the photon BEC, the strength of the photon-photon interaction has not yet been accurately measured, and even a full theoretical description is still lacking. Two mechanisms for interactions have been suggested: (i) the Kerr effect of intensity-dependent refractive index, and (ii) a temperature-dependent solvent refractive index, with temperature inhomogeneities driven by inhomogeneities of the light. Preliminary measurements indicated a dimensionless 2D interaction parameter of about $(7 \pm 3) \times 10^{-4}$ which is consistent with the second mechanism. However, this mechanism does not act at the single particle level, and is retarded, so may not have any effect on, for example, short-range particle correlations.

In this work, we derive an equation of motion for the pumped photon condensate in a dissipative microcavity, complete with effects of intensity-dependent refractive index, which leads to an effective photon-photon interaction. We use the equivalence of this equation to complex non-linear Schrödinger equations (cNLSEs) in other systems to help obtain the excitation spectrum and photoluminescence (PL) from the cavity, including the limited experimental resolution. We argue that the PL spectra is an excellent diagnostic for the photon-photon interaction strength. We propose an experimental apparatus for measuring the angle-resolved photoluminescence spectrum to an accuracy sufficient to determine interaction strength even as much as two orders of magnitude more precisely than current estimates.

Results

Equation of motion for a photon BEC The equation of motion for the condensate wavefunction of

*Correspondence should be addressed to r.nyman@imperial.ac.uk

a photon BEC in a dye-filled microcavity can be derived starting from Maxwell's equations in a non-linear medium (see Methods section). The cavity is so short that only one longitudinal mode is relevant, and the electric field of the light is oscillating at angular frequency ω . The equation of motion for the slowly-varying envelope of the electric field, $E_0(x, y)$ in a cavity whose length is $L_0 + \delta L(x, y)$ is:

$$\frac{1}{i\omega} \frac{\partial E_0}{\partial t} = \left[\left(\frac{\delta L}{L_0} - \frac{\delta\omega}{\omega} \right) + \frac{1}{k_L^2} \nabla_{\perp}^2 + \frac{3\chi^{(3)}}{2n_L^2} |E_0|^2 \right] E_0 - \frac{i}{2q\pi} \left[\left(\alpha - \beta |E_0|^2 \right) - (1-r) \right] E_0, \quad (1)$$

where $\chi^{(3)}$ is the Kerr non-linearity; $\delta\omega$ the cavity detuning; $k_L = 2\pi q/L_0 = \omega n_L/c$; n_L the refractive index in the limit of low light intensity; q the longitudinal mode number and α and β describe an incoherent pumping rate and saturation. The mirrors of the cavity have reflectivity r . Our co-ordinate system is summarised in Fig. 1. The non-linearity is assumed to be small, and the propagation of light is paraxial. Only the lowest relevant order in small quantities is retained. This equation describes only the condensed photons, and not the thermal (non-condensed) particles.

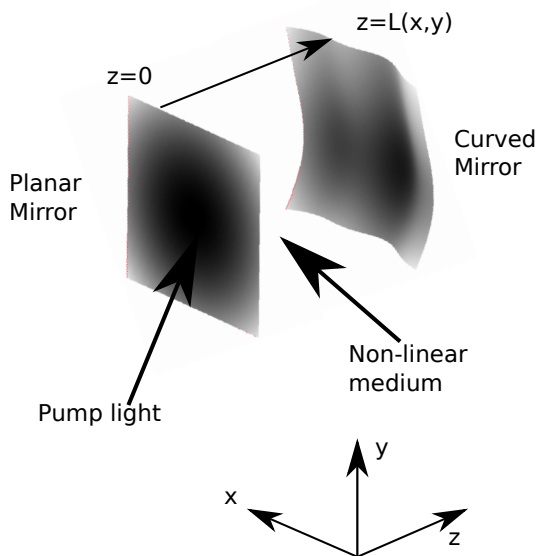


FIG. 1: A cavity filled with a non-linear medium which allows the photons to come to thermal equilibrium faster than they leave the cavity. The co-ordinate system is as used in the rest of this article. The length variations of the cavity play the role of a potential energy landscape for the photons. The cavity is so short that only one longitudinal mode is excited, and individual photons have a dispersion relation equivalent to that of massive particles.

Equivalence to a non-linear Schrödinger equation A typical form for the cNLSE for the condensate wavefunction ψ in a system with incoherent pumping (as

in photon BEC) is:

$$-i\hbar \frac{\partial \psi}{\partial t} = \left[V(\mathbf{r}) - \frac{\hbar^2}{2m} \nabla_{\perp}^2 + g|\psi|^2 + i(\gamma_{net} - \Gamma|\psi|^2) \right] \psi \quad (2)$$

where γ_{net} is the difference between the pump rate and cavity decay rate, and Γ describes the saturation of pumping (ensuring stability). In two dimensions $\int dx dy |\psi(x, y)|^2 = N_{BEC}$, where N_{BEC} is the number of particles in the condensate.

Comparing (1) and (2) the first term in Eqn. (1) is equivalent to potential energy in the cNLSE with an additional energy offset due to the detuning between the cavity mode and the light. The second term comes from diffraction of the light, and corresponds to kinetic energy, while the third term to the interactions. The energy stored in the electric field of the standing wave in the cavity is $\frac{1}{2} n_L^2 L_0 \epsilon_0 \int dx dy |E_0(x, y)|^2 = N_{BEC} \hbar \omega$. We can define the quantity m through $\hbar \omega = mc^2/n_L^2$, and this will play the role of an effective photon mass. With these analogies, we can convert the equation of motion for E_0 electric field Eqn. (1) into the cNLSE Eqn. (2) with the steady-state mean-field solution $\psi = \psi_0 e^{-i\mu t/\hbar}$ where μ is the chemical potential:

$$\psi_0 = E_0 \sqrt{\frac{n_L^2 \epsilon_0 L_0}{2\hbar \omega}} \quad (3)$$

$$g = \frac{3\hbar^2 \omega^2}{n_L^4 \epsilon_0 L_0} \chi^{(3)} = \frac{\hbar^2}{m} \tilde{g} \quad (4)$$

where \tilde{g} is the dimensionless 2D interaction parameter[16].

Excitation spectrum and photoluminescence

The incoherent photoluminescence (IPL) from the cavity, which can be measured by angle- and energy-resolved techniques, for a system in thermal equilibrium is given by the Bose-Einstein occupation function $n_B(\omega)$ times the spectral weight[17, 18]:

$$P_L(\mathbf{k}, \omega) = n_B(\omega) W(\mathbf{k}, \omega). \quad (5)$$

The spectral weight can be obtained from the retarded Green's function for the response of the system to perturbations, G_R :

$$W(\mathbf{k}, \omega) = 2 \text{Im} [G_R(\mathbf{k}, \omega)], \quad (6)$$

as shown for example in Ref. [19]. The exact form of G_R depends on the model used and here we determine G_R for a dissipative and driven case given by Eqn. (2) (the open system model) as well as for a simplified case where the dissipative terms are neglected (the closed system model). The two models give almost identical IPL since the decay processes in a photon BEC are very small. Thus we further use the closed system model to determine the influence of the trapping potential on IPL.

As described in the Methods section, the IPL from the dye-microcavity sample at temperature T using the open

system model of Eqn. (2) is

$$P_L^{(open)}(\mathbf{k}, \omega) = \frac{2\hbar}{e^{\hbar\omega/k_B T} - 1} \times \text{Im} \left[\frac{\mu + \epsilon_{\mathbf{k}} + \hbar\omega + i\hbar\gamma_{net}}{\hbar^2\omega(\omega + 2i\gamma_{net}) - \epsilon_{\mathbf{k}}(\epsilon_{\mathbf{k}} + 2\mu)} \right]. \quad (7)$$

The energy scale is relative to the chemical potential, so μ does not appear in distribution factor.

Fig. 2 shows the IPL energy-momentum spectrum, in which the Bogoliubov dispersion is clearly visible. The parameters of the calculation are experimentally achievable, and similar to values in Ref. [1]. For values of \tilde{g} above about 10^{-5} , the difference between free particles and photon quasiparticle excitations from the interacting condensate is very clear. Now by ignoring the dis-

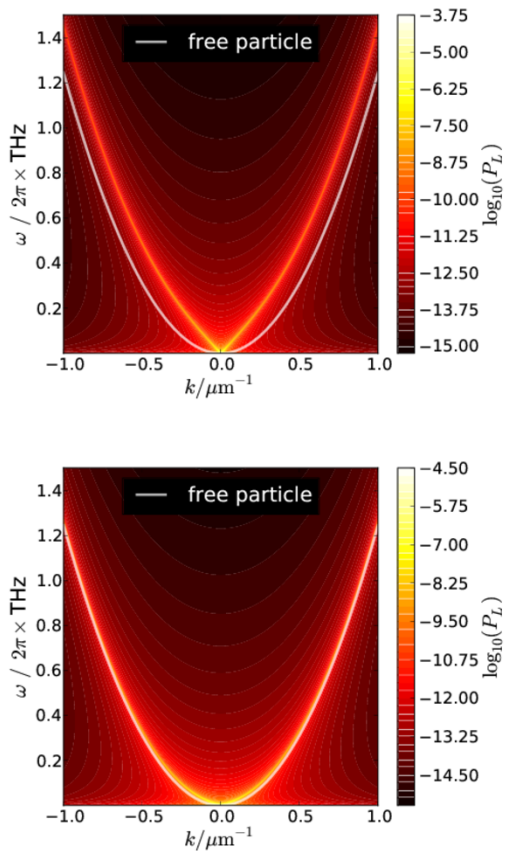


FIG. 2: Examples of photoluminescence, calculated using the open-system model. On this scale, the closed system results look the same. Top: dimensionless interaction parameter $\tilde{g} = 10^{-3}$ with 10^5 condensed photons. Bottom: $\tilde{g} = 10^{-5}$ and 10^5 condensed photons. As a guide for eye we plot the dispersion relation for free particle with the same photon mass. Angular frequency ω is taken relative to the chemical potential. Other parameters: $\gamma_{net} = 2\pi \times 1$ GHz; $T = 300$ K; central density calculated from Thomas-Fermi profile of photons in a circularly-symmetric harmonic trap of frequency 40 GHz.

sipative term in Eqn. (2) we determine the IPL for the

closed system. In the homogeneous case, the difference between the open- and closed-system models is mostly notable at low momentum and energy. The closed system follows the usual Bogoliubov modes down to zero momentum but the open system modes become diffusive at very low momenta[20–22]. However, the effects of interactions are observable in the IPL energy-momentum spectrum at moderate momenta and energy, and so the two models largely agree for the purposes of this work.

Photon BEC, however, is not homogeneous. In the local density approximation (LDA), we proceed by using a local chemical potential with $\mu'(\mathbf{r}) = \mu - V(\mathbf{r})$. The energy spectrum for excitations is $\xi_{\mathbf{k}}(\mathbf{r}) = \sqrt{\epsilon_{\mathbf{k}}(\epsilon_{\mathbf{k}} + 2\mu'(\mathbf{r}))}$. This is a local version of the Bogoliubov spectrum[23]. There are finite temperature corrections[24] which we are neglecting here. The local spectral weight is then given by:

$$W^{(closed)}(\mathbf{k}, \omega; \mathbf{r}) = \frac{\epsilon_{\mathbf{k}} + \mu'(\mathbf{r}) + \xi_{\mathbf{k}}(\mathbf{r})}{2\xi_{\mathbf{k}}(\mathbf{r})} \delta(\hbar\omega - \xi_{\mathbf{k}}(\mathbf{r})) - \frac{\epsilon_{\mathbf{k}} + \mu'(\mathbf{r}) - \xi_{\mathbf{k}}(\mathbf{r})}{2\xi_{\mathbf{k}}(\mathbf{r})} \delta(\hbar\omega + \xi_{\mathbf{k}}(\mathbf{r})). \quad (8)$$

The energy scale is shifted such that excitations of energy $\hbar\omega = 0$ are at the chemical potential. Some broadening is put into the system by hand by adding an imaginary part $\hbar\kappa$ to the energy, $\epsilon \rightarrow \epsilon - i\hbar\kappa$ and, when integrated around the zero of the argument, $\delta(\epsilon) \rightarrow \frac{1}{\pi} \frac{\hbar\kappa}{\epsilon^2 + \hbar^2\kappa^2}$. The local Bose occupation factor becomes $n_B(\omega; \mathbf{r}) = \frac{\hbar}{e^{[\hbar\omega - V(\mathbf{r})]/k_B T} - 1}$ where $n_B(\omega) = \iint d^2\mathbf{r} n_B(\omega; \mathbf{r})/A$ and A is a typical area of the system, e.g. $2\pi\mu/m\Omega_0^2$ for in the Thomas-Fermi limit in a harmonic potential. The total photoluminescence observable becomes:

$$P_L^{(closed)}(\mathbf{k}, \omega) = \iint d^2\mathbf{r} n_B(\omega; \mathbf{r}) W^{(closed)}(\mathbf{k}, \omega; \mathbf{r}). \quad (9)$$

An inhomogeneous confining potential means that the density varies across the condensate, which in turn leads to variations in the Bogoliubov spectrum, i.e. the speed of sound. The integration over all positions of the condensate causes the lines in the IPL energy-momentum spectrum to broaden, making it more difficult to see the effects of interactions. The photoluminescence calculated here is the incoherent part; coherent photoluminescence will be emitted from the condensate mode. It may contain a large range of momenta, but it will all be at the lowest energy available, and so incoherent and coherent light can easily be distinguished (condensate broadening in energy is expected to be very small on the scale of Fig. 2)

Energy-momentum spectroscopy It is possible to observe the photoluminescence resolved in both energy and one component of momentum. The angle-resolved photo-emission spectrum (ARPES) of exciton-polariton samples has been successfully measured, demonstrating the effect of interactions on the Bogoliubov dispersion

relation[5, 6]. The basic experimental optical apparatus to be used for photon BEC ARPES is shown in Fig. 3.

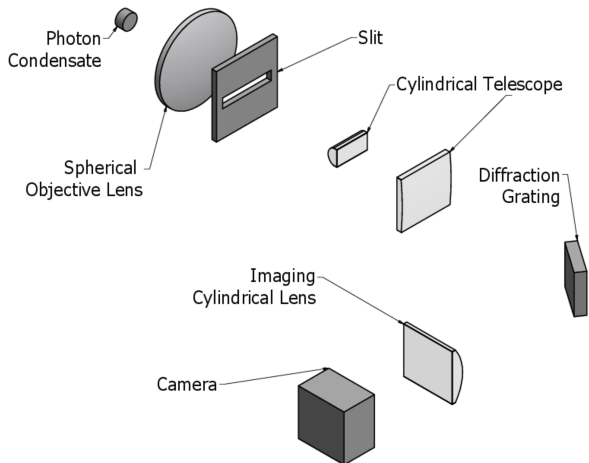


FIG. 3: A schematic diagram of Angle-Resolved Photo-Emission Spectroscopy (ARPES). Photoluminescence from the photon condensate is collimated by the (spherical) objective lens. Components with wavenumbers $k_y \simeq 0$ only pass through the slit. A cylindrical telescope magnifies the light in the y -direction, before it strikes a reflective diffraction grating, whose rules run parallel to the x -direction. The (cylindrical) imaging lens then ensures that the image on the camera corresponds to momentum (x) and energy (y).

The angle of a photon relative to the optic axis inside the cavity is $\theta_{int} = (\theta_x, \theta_y) = \arctan(\mathbf{k}/k_0)$ with $k_0 = q\pi n_L/L_0$ being the typical wavenumber. The angle that the emitted light makes to the optic axis is then $\theta_{ext} = \arcsin(n_L \sin \theta_{int})$. The photoluminescence is at the focus of the objective lens of focal length f_{obj} , and so the displacement from the optic axis is $(x, y) = n_L f_{obj} \mathbf{k}/k_0$ (in the small angle approximation). Behind the objective, the light passes through a slit of size d_{slit} in the y direction so only the $k_y \simeq 0$ components make it through. The image in momentum space is unaffected by subsequent optics. In order to improve spectral resolution, the image is magnified in the y direction by a cylindrical telescope of magnification M_y and it strikes a reflective grating, whose lines are parallel to the x direction and spaced by $d_{grating}$ in y . The first-order diffraction angle in the y direction is $\theta_y = \arcsin(\lambda/d_{grating})$, with λ being the wavelength of light. The light passes through a cylindrical imaging lens of focal length f_{im} , and the camera sits at this focus.

Experimental limits to measuring interactions

The mapping between (k_x, λ) and position on screen is blurred by diffraction in the propagation of the light from source to detector. We analyse what the minimum resolvable momentum and energy would be, and what that means for the minimum resolvable interaction strength. In general, interactions will be detectable when the Bogoliubov spectrum is significantly different from the free-particle spectrum. This happens on energy scales less than $\xi_{min} \simeq 2\mu$, and momentum scales less

than $p_{min} \simeq 2\sqrt{m\mu}$.

The monochromator optics for energy resolution means that the Fourier-space image (after the objective lens and slit) will propagate and diffract before it reaches the camera. The propagation distance between objective lens and camera is L_{prop} . A range of small transverse wavenumbers δ_k corresponds to a region of size $n_L f_{obj} \delta_k/k_0$ at the objective, which will diffract to a region of size $\delta_x^{(cam)} = 2L_{prop}/n_L f_{obj} \delta_k$ at the camera (in the far field). Inverting this expression gives the diffraction limit for transverse wavenumber. Considering the mapping between angle and position, the equivalent limit set by the pixel size δ_x^{px} of the camera is $\delta_k/k_0 = \delta_x^{(px)}/n_L f_{obj}$. The optimum results will be achieved with diffraction limit roughly equal to pixelisation limit, and we find:

$$\delta_k^{(min)} = \frac{2}{n_L f_{obj}} \sqrt{\frac{\pi L_{prop}}{\lambda}}. \quad (10)$$

The same analysis yields an optimal pixel size of $\delta_x^{(px)} = \sqrt{L_{prop} \lambda / \pi}$. Putting in plausible experimental values $f_{obj} = 0.2$ m, $L_{prop} = 0.3$ m and $\lambda = 580$ nm, we obtain a minimum in-plane momentum resolution of $1.3 \times 10^4 \text{ m}^{-1}$. The appropriate camera pixel size would be about $180 \mu\text{m}$, which is trivially achievable. It is clearly advantageous to use a long focal length objective: to collimate a useful range of momenta, a lens with $f_{obj} = 0.2$ m should be 20 mm diameter. The equivalent size of the slit in momentum space should be no bigger than the expected momentum resolution of the entire optical system. In real space, that means that the slit should be about the same size as the detector pixels, $d_{slit} \sim 180 \mu\text{m}$.

Energy resolution is limited by the size of the beam at the grating. The resolving power for the first-order diffraction fringe is approximately equal to the number of grating lines covered by the incident beam: $\delta_\lambda = \lambda d_{grating}/D$. Reasonable experimental parameters are $1/d_{grating} = 900$ lines/mm and $D = d_{slit} M_y = 18$ mm (implying a cylindrical telescope of magnification approximately 75). The resulting wavelength resolution is $\delta_\lambda = 0.04$ nm, or equivalently $\delta_\epsilon = h \times 30$ GHz for 580 nm emission. With an imaging lens focal length of $f_{im} = 50$ mm, the detector pixel size required not to compromise this resolution is $4 \mu\text{m}$: a commonplace pixel size for a CCD camera.

Minimum detectable interaction strength

For reasonable parameters of $\Omega_0 = 2\pi \times 40$ GHz and $N_{BEC} = 10^5$, and optics as previously described, we find that it should be possible to resolve interactions as weak as $\tilde{g}_{min} \simeq \left(\frac{\hbar^2 \delta_k^2}{4m}\right)^2 \frac{\pi}{N_{BEC} (\hbar\Omega_0)^2} = 2 \times 10^{-10}$ (if momentum is the limiting resolution) or $\tilde{g}_{min} \simeq \delta_\epsilon^2 \frac{\pi}{N_{BEC} (2\hbar\Omega_0)^2} = 2 \times 10^{-5}$ (if energy resolution is the limiting factor). It is worth noting that for extremely weak interactions, the Thomas-Fermi approximation used in deriving the photoluminescence spectrum is unlikely to be very accurate.

Discussion

The implication for the experimenter is that the momentum is easily resolved, so most experimental effort will be required to attain the best possible energy resolution. Interactions 40 times weaker than those reported in Ref. [1] should be detectable. Advanced data analysis could further improve the sensitivity. An example of plausible experimental data is shown in Fig. 4, which includes both energy and momentum instrumental broadening and the effects of saturation and finite dynamic range of the detector camera (noise is not included in the model).

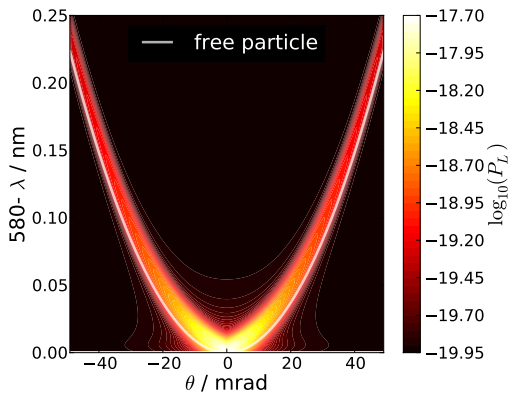


FIG. 4: Observable photoluminescence energy-momentum spectrum using a closed-system model, including the effects of the inhomogeneous confining potential, finite instrumental resolution in momentum and energy, and the finite dynamic range of a typical camera. Experimental parameters are described in the main text. Dimensionless interaction strength, number of condensed photons, temperature and trap frequency are 10^{-5} , 10^5 , 300 K and 40 GHz respectively.

If the energy resolution required cannot be matched by grating spectroscopy, then an external Fabry-Perot cavity spectrometer would be a viable alternative. The minimum energy resolution in that case would most likely be set by the intrinsic linewidth of the resonator which contains the photon condensate, probably about 1 GHz. The limit on \tilde{g} would in that case be somewhere around 10^{-6} .

There is very little literature on the non-linear susceptibility of dyes like Rhodamine. The closest available data is for very short pulses, which gives an underestimate of the non-linearity since the steady-state excited state population has not been reached. Taking a reasonable value for the scattering cross-section of Rhodamine[25] of $2 \times 10^{-22} \text{ m}^2$, and using the result of Ref. [26], we infer $\chi^{(3)} \simeq 5 \times 10^{-20} (\text{m/V})^2$. This in turn implies a lower bound for the 2D dimensionless interaction parameter: $\tilde{g} > 2 \times 10^{-7}$.

The intensity-dependent refractive index may come from an effect as simple as saturation of the excited state

population. For two-level systems, at short wavelengths one expects negative $\chi^{(3)}$ leading to repulsive interactions, but attractive interactions for long wavelengths. This frequency-dependent (i.e. also time-dependent) interaction strength leaves open the possibility for retarded interactions which will complicate the analysis of excitations about the condensate, and could lead to so-far unpredicted phenomena.

To conclude, we believe that the photoluminescence spectrum from a photon BEC can be observed using standard optical elements (lenses, a diffraction grating and a camera), with a sufficient resolution to detect dimensionless interaction parameters as small as about 10^{-5} . If a Fabry-Perot resonator were used, the resolution may be an order of magnitude better. This compares well to the best available data in the literature on non-linear susceptibilities in Rhodamine dyes, and we can expect interaction effects in photon BECs to be experimentally observed via the energy-momentum spectrum.

Methods

Derivation of the equation of motion for photon BEC

We start from Maxwell's equations in a non-magnetic, dielectric medium with a non-linear electric polarisability and propagate the wave from one mirror of the cavity to the other and back again. The net change in electric field over one cycle of propagation divided by the time that cycle takes determines the time derivative for the electric field. Note, that it is also possible to obtain a similar equation of motion by considering a decomposition over quasi-normal modes of the optical resonator in appropriate paraxial and slowly-varying-envelope approximations [27].

The non-linear electric polarisability of the medium can be accounted for by writing the electric polarisation as a linear part plus a non-linear part[28]: $\mathbf{P} = \mathbf{P}_L + \mathbf{P}_{NL}$. The constitutive relation is $\mathbf{D} = \epsilon_0 \epsilon_L \mathbf{E} + \mathbf{P}_{NL}$, where the linear permittivity (in the limit of low intensity light) is $\epsilon_L = n_L^2 = 1 + \chi_L$ and χ_L is the linear susceptibility. We define n_L as the refractive index at low intensity, and the wave equation for the electric field becomes:

$$\nabla(\nabla \cdot \mathbf{E}) - \nabla^2 \mathbf{E} + \frac{n_L^2}{c^2} \ddot{\mathbf{E}} = -\frac{1}{c^2} \ddot{\mathbf{P}}_{NL} \quad (11)$$

with the dot representing the time derivative. We make the paraxial approximation and assume that the electric field can be written as a scalar (constant polarisation throughout space, perpendicular to the direction of propagation). We consider a travelling wave solution, $E = E_0(x, y, z)e^{i(k_L z - \omega t)}$ with a slowly-varying envelope: z is the axis of the optical resonator. For annotation's sake, where only one argument of E_0 is given, it is z ; x and y are left implicit. With two arguments, they are x and y , leaving $z = 0$ implicit. The angular frequency and wavenumber of the light are ω and $k_L = \omega n_L / c$ respectively. Now, using conventional definitions for the Kerr-type non-linearity, the paraxial wave equation becomes:

$$-\left\{ 2ik \frac{\partial E_0}{\partial z} + \frac{\partial^2 E_0}{\partial z^2} + \nabla_{\perp}^2 E_0 \right\} = \frac{k_L^2}{n_L^2} 3\chi^{(3)} |E_0|^2 E_0 \quad (12)$$

where $\nabla_{\perp}^2 = \frac{\partial^2}{\partial x^2} + \frac{\partial^2}{\partial y^2}$. Starting from the electric field at $z = 0$, we can find the field some small propagation distance away at $z = L$ using a first-order Taylor expansion:

$$E_0(L) \simeq E_0(0) - \frac{L}{2ik_L} \left\{ \nabla_{\perp}^2 E_0(0) + \frac{k_L^2}{n_L^2} 3\chi^{(3)} |E_0(0)|^2 E_0(0) \right\}. \quad (13)$$

We now consider a forward travelling wave with an electric field envelope $E_0^{\rightarrow}(x, y, 0)$ and use Eqn. (13) to find the electric field at the other mirror. We will allow the mirror surface position to vary, so the cavity length is a function of position: $L(x, y) = L_0 + \delta L(x, y)$. For length variations are much less than the wavelength of the light, we make a linear approximation for the phase of the light, and neglect additional envelope propagation effects. The forward propagating field at the second mirror is:

$$E_0^{\rightarrow}(x, y, L(x, y)) = E_0^{\rightarrow}(0) \left(e^{-ik_L L_0} + ik_L \delta L \right) \quad (14)$$

$$- \frac{L_0}{2ik_L} e^{ik_L L_0} \left\{ \nabla_{\perp}^2 E_0^{\rightarrow}(0) + \frac{k_L^2}{n_L^2} 3\chi^{(3)} |E_0^{\rightarrow}(0)|^2 E_0^{\rightarrow}(0) \right\}.$$

The mirrors have transmission and reflectance τ and r respectively. After reflection, the backwards propagating field at $L(x, y)$ is $E_0^{\leftarrow}(L(x, y)) = -r E_0^{\rightarrow}(L(x, y))$. Propagation to the first mirror at $z = 0$ and subsequent reflection follow the same pattern. Finally, to complete a cycle, inhomogeneous pump light enters through the mirror at $z = 0$. In order to model saturable, incoherent pumping, it is sufficient to write the pump term in the form $(\alpha - \beta |E_0|^2) E_0$. Here, α represents gain via stimulated scattering of photons into the condensate, and β governs saturation[29].

The time taken for a cycle is given by $\delta t = c/2n_L L_0$, where c is the speed of light in vacuum. The electric field change δE_0 in one cycle is derived as above, and then we convert finite differences to derivatives: $\delta E_0/\delta t = \frac{\partial E_0}{\partial t} = \dot{E}_0$. High-order terms in small quantities are neglected. The equation of motion for the electric field envelope at the first mirror, assuming that it varies slowly compared to the cavity round-trip time becomes Eqn. (1).

Finally, it is straightforward to include the effects of inhomogeneous linear refractive index (which appears as an increase in the effective length of the cavity), or spatially variable mirror reflectivities.

Retarded Green's function In the homogeneous case, $V(x, y) = 0$, the steady-state mean-field solution of Eqn. (2) ψ_0 , is found, by writing a solution with time variation $e^{-i\mu t/\hbar}$ to obtain the chemical potential $\mu = g|\psi_0|^2$. Note that in the Thomas-Fermi limit of a harmonic trap with frequency Ω_0 , the chemical potential is $\hbar\Omega_0\sqrt{\frac{g}{\pi} \frac{N_{BEC}}{\pi}}$. The equation of motion for small (linear) variations about this mean field, $\delta\psi$ can be obtained by starting from a total wavefunction as $\psi = \psi_0 + \delta\psi$ and subtracting the mean-field solution:

$$-i\hbar \frac{\partial}{\partial t} \delta\psi = \left[-\frac{\hbar^2}{2m} \nabla_{\perp}^2 + 2g|\psi_0|^2 \right] \delta\psi + [g\psi_0^2] \delta\psi^*. \quad (15)$$

Comparison with the Hermitian conjugate leads to a system of linear equations in $\delta\psi$ and $\delta\psi^*$. The matrix operator which relates the two is the inverse Green's function[17], $(\mathcal{G})^{-1}$, which is also known as the Bogoliubov operator[22]:

$$-i\hbar \frac{\partial}{\partial t} \begin{pmatrix} \delta\psi \\ \delta\psi^* \end{pmatrix} = (\mathcal{G})^{-1} \begin{pmatrix} \delta\psi \\ \delta\psi^* \end{pmatrix}. \quad (16)$$

In the stationary and homogeneous case, the inversion is most easily performed in Fourier space to give [6]:

$$\mathcal{G}_{\mathcal{R}}(\mathbf{k}, \omega) = \frac{1}{\hbar^2\omega(\omega + 2i\gamma_{net}) - \epsilon_{\mathbf{k}}(\epsilon_{\mathbf{k}} + 2\mu)} \times \quad (17)$$

$$\begin{pmatrix} \mu + \epsilon_{\mathbf{k}} + \hbar\omega + i\hbar\gamma_{net} & -\mu + i\hbar\gamma_{net} \\ -\mu - i\hbar\gamma_{net} & \mu + \epsilon_{\mathbf{k}} - \hbar\omega + i\hbar\gamma_{net} \end{pmatrix}$$

where $\epsilon_{\mathbf{k}} = \frac{\hbar^2 k^2}{2m}$ is the kinetic energy of a free particle, and \mathbf{k} is in the x, y plane. The relevant component for the photoluminescence is the diagonal $(\delta\psi, \delta\psi)$ component of the full Green's function: $\mathcal{G}_{\mathcal{R}}(\mathbf{k}, \omega) = \mathcal{G}_{\mathcal{R}}^{11}(\mathbf{k}, \omega)$.

-
- [1] J. Klaers, J. Schmitt, F. Vewinger, and M. Weitz, *Nature* **468**, 545? (2010).
- [2] J. Klaers, F. Vewinger, and M. Weitz, *Nature Physics* **6**, 512 (2010).
- [3] P. Kirton and J. Keeling, arXiv preprint arXiv:1303.3459 (2013).
- [4] J. Kasprzak, M. Richard, S. Kundermann, A. Baas, P. Jeambrun, J. Keeling, M. FM Marchetti, *et al.*, *Nature* **443**, 409 (2006).
- [5] S. Utsunomiya, L. Tian, G. Roumpos, C. Lai, N. Kumada, T. Fujisawa, M. Kuwata-Gonokami, A. Löffler, S. Höfling, A. Forchel, *et al.*, *Nature Physics* **4**, 700 (2008).
- [6] G. Roumpos, M. Lohse, W. H. Nitsche, J. Keeling, M. H. Szymańska, P. B. Littlewood, A. Löffler, S. Höfling, L. Worschech, A. Forchel, and Y. Yamamoto, *Proceedings of the National Academy of Sciences* **109**, 6467 (2012).
- [7] K. G. Lagoudakis, M. Wouters, M. Richard, A. Baas, I. Carusotto, R. André, L. S. Dang, B. Deveaud-Plédran, *et al.*, *Nature Physics* **4**, 706 (2008).
- [8] D. Sanvitto, F. Marchetti, M. Szymańska, G. Tosi, M. Baudisch, F. Laussy, D. Krizhanovskii, M. Skolnick, L. Marrucci, A. Lemaître, J. Bloch, C. Tejedor, and L. V. na, *Nature Physics* **6**, 527 (2010).
- [9] P. Cristofolini, A. Dreismann, G. Christmann, G. Franchetti, N. G. Berloff, P. Tsotsis, Z. Hatzopoulos, P. G. Savvidis, and J. J. Baumberg, *Phys. Rev. Lett.* **110**, 186403 (2013).
- [10] R. Y. Chiao and J. Boyce, *Phys. Rev. A* **60**, 4114 (1999).
- [11] E. L. Bolda, R. Y. Chiao, and W. H. Zurek, *Phys. Rev. Lett.* **86**, 416 (2001).
- [12] A. Tanzini and S. Sorella, *Physics Letters A* **263**, 43 (1999).
- [13] L. A. Lugiato and R. Lefever, *Phys. Rev. Lett.* **58**, 2209 (1987).
- [14] M. Brambilla, L. A. Lugiato, V. Penna, F. Prati, C. Tamm, and C. O. Weiss, *Phys. Rev. A* **43**, 5114 (1991).
- [15] K. Staliunas, *Phys. Rev. A* **48**, 1573 (1993).
- [16] Z. Hadzibabic and J. Dalibard, *Rivista del Nuovo Cimento* **34**, 389 (2011), see also the ArXiv version <http://arxiv.org/abs/0912.1490>.
- [17] F. M. Marchetti, J. Keeling, M. H. Szymańska, and P. B. Littlewood, *Phys. Rev. B* **76**, 115326 (2007).
- [18] M. H. Szymańska, J. Keeling, and P. B. Littlewood, *Phys. Rev. B* **75**, 195331 (2007).
- [19] J. Keeling, P. R. Eastham, M. H. Szymanska, and P. B. Littlewood, *Phys. Rev. B* **72**, 115320 (2005).
- [20] M. H. Szymańska, J. Keeling, and P. B. Littlewood, *Phys. Rev. Lett.* **96**, 230602 (2006).
- [21] M. Wouters and I. Carusotto, *Phys. Rev. A* **76**, 043807 (2007).
- [22] I. Carusotto and C. Ciuti, *Rev. Mod. Phys.* **85**, 299 (2013).
- [23] P. O. Fedichev and G. V. Shlyapnikov, *Phys. Rev. A* **58**, 3146 (1998).
- [24] L. Pitaevskii and S. Stringari, *Bose-Einstein Condensation* (Oxford University Press, Oxford, 2003).
- [25] *Dye Lasers*, edited by F. Schaefer (Springer-Verlag, Berlin, 1990).

- [26] S. Delysse, J.-M. Nunzi, and C. Scala-Valero, *Applied Physics B* **66**, 439 (1998).
- [27] L. A. Lugiato and C. Oldano, *Phys. Rev. A* **37**, 3896 (1988).
- [28] R. Boyd, *Nonlinear optics*, 3rd ed. (Academic Press, , 2008).
- [29] J. Keeling and N. G. Berloff, *Phys. Rev. Lett.* **100**, 250401 (2008).

Acknowledgements We are grateful to EPSRC for funding this work (RAN for the fellowship EP/J017027/1

and MHS under fellowship EP/K003623/1 and grant EP/I028900/1). We thank Jan Klaers, Jonathan Keeling and Peter Kirton for informative discussions.

Author contributions These calculations came about while setting up an experimental photon BEC effort. RAN set up the experimental problem, and MHS knocked it down with the theoretical foundation. We wrote the article together.